23rd Australasian Fluid Mechanics Conference – 23AFMC
Sydney, Australia
4-8 December 2022
Paper No: AFMC2022-126

Effect of pressure tap density on prediction of wind-induced loads and dynamic response of tall buildings

M. Mahdi Salehinejad [1*], Yin Fai Li [1], Quincy Ma [2] and Richard George James Flay [1]

[1] Department of Mechanical and Mechatronics Engineering, Faculty of Engineering, University of Auckland, Auckland, 1023, New Zealand

[2] Department of Civil and Environmental Engineering, Faculty of Engineering, University of Auckland, Auckland, 1023, New Zealand

* Email: msal381@aucklanduni.ac.nz

Abstract

The high frequency pressure integration method is one of the most accurate approaches for obtaining wind loads on tall buildings in wind tunnel investigations. In this technique, simultaneous time histories of the pressures at hundreds of taps on the surface of rigid building models are recorded. To reach acceptable accuracy in the predictions of wind-induced loads and dynamic response in this approach, the resolution of pressure taps on the building area should be fine enough to capture the spatial distribution of the pressures. However, the complexity of the geometry and model size of the buildings may provide limited space to install the associated tubing inside the model. Thus, there will be a practical limit on the maximum number of taps that can be installed. In this study, the influence of pressure tap resolution on the prediction of wind-induced loads and dynamic response are examined for Building A, a benchmark tall building [1, 2]. The effect on response predictions from different pressure tap layout densities on the rigid model is examined and compared with the recommendations from the Australasian Wind Engineering Society Quality Assurance Manual [3]. Time-averaged pressure coefficient distributions for a range of pressure tap layout densities are illustrated. From these distributions, time histories of base shears and bending moments and torsion are calculated and compared from the various pressure tap densities. Dynamic responses including sway and twist moments, acceleration and displacement are predicted using time domain analysis to investigate the effect of pressure tap resolution. It is found that horizontal tap density has significantly more effect than vertical spacing on the predictions of wind-induced loads and dynamic response.

1. Introduction

In the present day, tall buildings are considered wind-sensitive structures. In fact, due to enhanced flexibility of modern tall buildings and high design wind speeds, they are vulnerable to wind loads [4]. Thus, accurate predictions of wind loads and wind responses of such structures are needed. Wind tunnel testing is the favourite option to measure the wind loads on tall building rigid models. To achieve this goal, the High-Frequency Force Balance (HFFB) and High-Frequency Pressure Integration (HFPI) approaches are widely used as reliable experimental techniques [4, 5]. The HFFB approach measures overturning moments, torsion, and shears at the base of rigid building models, while the HFPI approach can measure and record simultaneously pressures at hundreds of taps on the surface of rigid building models [6]. Each technique offers advantages as well as disadvantages. The HFPI method provides more accurate wind-induced loads and dynamic response results. Using the HFPI approach, it is possible to consider the higher modes and complex mode effects easily, compared to the HFFB approach [4, 7]. However, the HFPI method requires intensive pressure tap densities on the outer surfaces of the building models. It poses more labourintensive works needing determination of tributary areas, moment and torsion arms and the installation of hundreds of pressure taps [8].

To reach satisfactory accuracy in the estimations of wind-induced loads and dynamic response in the HFPI approach for strength and serviceability design, the resolution of pressure taps on the building area should be fine enough to capture the spatial distribution of the pressures. Nevertheless, the complexity of the geometry and model size of the tall buildings may provide only limited space to install the associated tubing inside the rigid model. Thus, there will be a practical limit on the maximum number of taps that can be installed. This importance makes the pressure tap density and configuration key to defining the HFPI method performance [6].

The Australasian Wind Engineering Society Quality Assurance Manual recommends a maximum full-scale area of 120 m^2 per tap for strength design [3]. Tokyo Polytechnic University (TPU) database utilises pressure taps with 64 m^2 average tributary area [6, 9]. However, there is no recommendation provided by ASCE 49-12 Standard [10] on pressure tap density. Dragoiescu et al. [8] conducted HFFB and HFPI wind tunnel studies to compare base moments and torsion obtained with these two techniques. To carry out the HFPI wind tunnel tests, they used the standard CAARC (Commonwealth Advisory Aeronautical Council) tall building rigid model [11] with almost 100 m^2 average tributary area per tap. Although there were some differences in r.m.s. values for the across-wind base moments and mean values of torsion at some specific wind direction, the results from both approaches showed good agreement. In another study, Dragoiescu et al. [12] carried out wind tunnel studies to examine the effect of tap resolution on the standard CAARC model. They found that a very high density was required for acquiring accurate results while horizontal tap resolution is more significant than vertical resolution, especially in the case of the torsional moment. It is necessary to say that they did not explore the pressure tap resolution effects on the dynamic response of the building. In a comprehensive investigation, Park and Yeo [6] examined the effect of pressure tap density and configuration on wind-induced loads and dynamic response of a specific tall building. They defined 16 cases of pressure tap layout for their square-plan-shape tall building. By scrutinising pressure distributions, time histories of sway moments and torsion, inter-story drift ratios and resultant floor acceleration, their research emphasised that the results are more sensitive to horizontal tap density variations than vertical tap density variations. Also, the base torsional moments showed the highest sensitivity to the pressure tap density and configuration.

In this HFPI wind tunnel study, the influence of pressure tap resolution on the prediction of wind-induced loads and dynamic response are examined for Building A, a wind engineering benchmark tall building [1, 2]. The effect of four pressure tap layout densities on the rigid model is studied and compared with the literature such as the recommendations from the Australasian Wind Engineering Society Quality Assurance Manual [3]. Time-averaged pressure coefficient distributions for a range of pressure tap layout densities are illustrated. Tributary areas for pressure taps, moment and torsion arms are defined separately for each case. From the pressure distributions, time histories of base shears and bending moments and torsion are calculated and compared from the various pressure tap densities. Dynamic responses including sway and twist moments, tip acceleration and tip displacement are estimated using time domain analysis to explore the effect of pressure tap density.

2. Experimental setup

Wind tunnel tests were carried out in the closed circuit boundary layer wind tunnel of the University of Auckland. It has a working section of 3.6 m × 2.5 m and a maximum speed of 20 m/s. To simulate the specified [1,2] turbulent wind field, a combination of triangular shaped spires and arrayed roughness elements with different sizes were placed on the tunnel floor at the entrance to the test section. The configuration used gave a suburban terrain flow simulation. A high sensitivity velocity measuring device, a multi-hole probe (Cobra probe), was used to obtain the flow fluctuations. The mean wind speed profile of the boundary layer flow was found to follow a power law with an exponent $\alpha = 0.25$ and a value of 0.2 m for the roughness length. This is consistent with Terrain Category 3 (TC3) as specified in the Standard AS/NZS 1170.2 [13]. The mean velocity profile normalised by the velocity at a reference height of 800 mm (which represents the top of the target tall building model), and the turbulence intensity profile are displayed in Figure 1 with the target profiles from AS/NZS 1170.2 for TC3. The mean wind speed and turbulence intensity profiles should fall within ±10% of the target profiles [1, 2]. Figure 1 shows good agreement between measured and target values. There are some values close to the ground with more than ±10% error, which is an acceptable experimental error for very low heights because of their less contribution to wind loads compared to higher heights [7]. It is worth noting that the longitudinal velocity spectrum of the simulated wind flow agrees well with the von Karman-type spectrum.

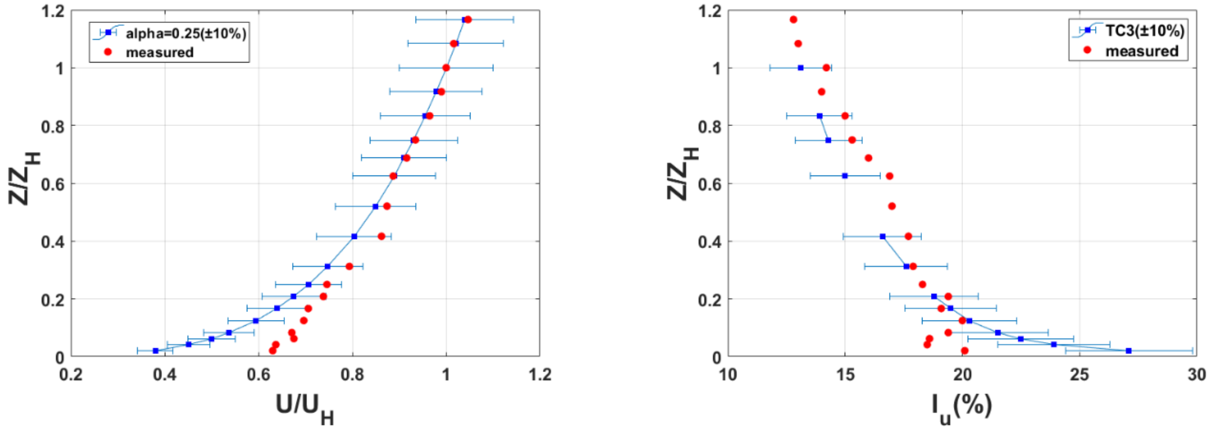

a b

Figure 1. a) Mean wind speed profiles, b) Turbulence intensity profiles [14].

Building A, a benchmark tall building [1, 2] is used in this study. It is 240 m high and has a rectangular cross-section with dimensions of 72 m by 24 m. The dynamic modes are non-linear and incorporate lateral-torsional coupling. The sway frequencies are 0.231 Hz and 0.492 Hz for the principal orthogonal axes of the building. The twist frequency is 0.536 Hz. The structural damping ratio has been chosen as 2.5 % for this building. Also, the centres of mass for different levels are offset from the geometric centre. A rigid model of this building was made of transparent plexiglass at a scale of 1:300. To permit thorough pressure measurements, 396 pressure taps were instrumented on the four surfaces of the model. Pressure data were acquired at a sampling frequency of 400 Hz with a sampling period of 120 s for each wind tunnel test. The model was installed at the centre of the wind tunnel turntable to allow testing in different wind flow directions. This study focuses on three wind directions: 0°, 40°, and 90°. The boundary layer wind tunnel configuration with the pressure-tapped model in the foreground can be seen in Figure 2a. Additionally, Figure 2b demonstrates the global reference system and the definition of wind direction in the wind tunnel tests.

a b

Figure 2. a) Boundary layer wind tunnel setup with HFPI rigid model, b) Global reference system of the tests [14].

3. Methodology

3.1 Pressure tap layouts

Pressure distributions across 396 taps are obtained using the electronical pressure scanner built in-house by the department of mechanical engineering, the University of Auckland. The taps are arranged with 22 pressure taps at 18 levels. All pressure tubes have 1 m length, and the measurement frequency was 400 Hz. This means that the model has 126 pressure taps on each wide façade and 72 pressure taps on each narrow façade. This arrangement of pressure taps over the model surface is shown in Figure 3a. Based on this maximum density pressure tap layout (case 1), three additional layouts are defined using vertical and horizontal variations (Figure 3) by discarding data from specific taps in post processing of wind tunnel data. Case 2 has nine levels with 22 pressure taps on each level. Case 3 has 18 levels with 11 pressure taps on each level. Case 4 has nine levels with 11 pressure taps on each level.

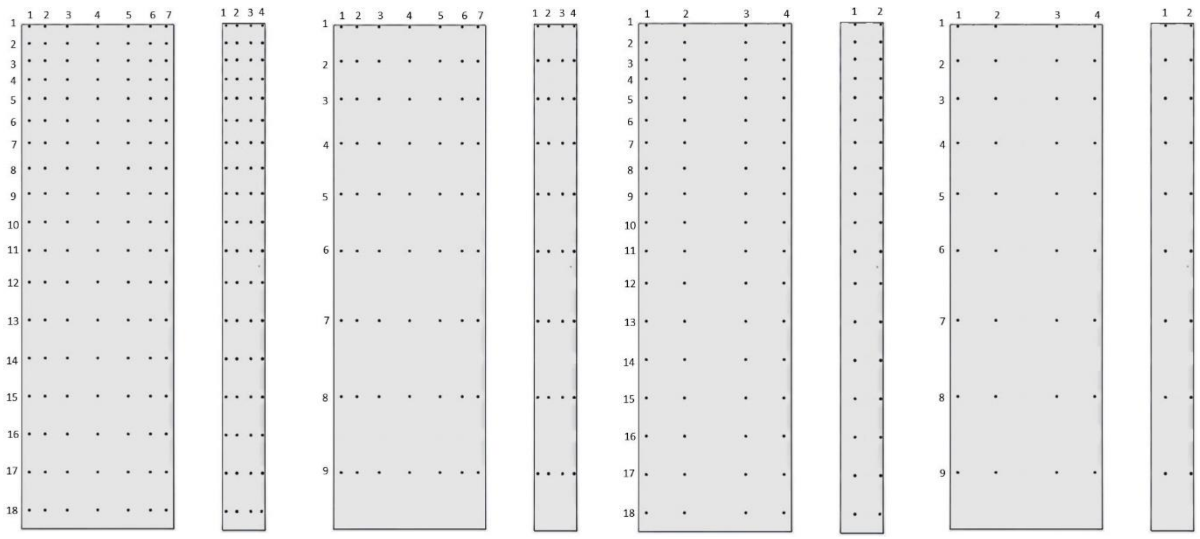

Figure 3. The four pressure tap layouts: a) Case 1 (18×22), b) Case 2 (9×22), c) Case 3 (18×11), d) Case 4 (9×11).

It is obvious that the highest pressure tap density is case 1, while case 4 has the lowest density. The pressure tap resolutions and average pressure tap densities in these four cases are summarised in Table 1.

	Vertical tap variation	Horizontal tap variation	Total pressure tap number	Average area per pressure tap (m^2)
Case 1 (original)	18	22	396	116
Case 2	9	22	198	233
Case 3	18	11	198	233
Case 4	9	11	99	465

Table 1. Pressure tap layout information for 4 cases.

3.2 Wind-induced loads and moments

The fluctuating wind loads on the building are derived from surface pressure distribution measurements. Local pressure coefficients from the wind tunnel measurements were calculated using the following equation:

$$C_{p_{ij}} = \frac{p_{ij}(t) - p_\infty}{0.5\rho U_h^2} \quad (1)$$

Here, i=1,2, …,18 denotes the pressure tap layer and j=1,2, …,22 indicates the pressure tap number in each level, p_∞ is the local static pressure, ρ is the air density, and U_h is the wind speed at the top of the building, which was 9 m/s for the wind tunnel tests. Using the pressure coefficients for each of the pressure tap layout cases allows the time-averaged pressure coefficient distributions for the four cases to be calculated.

To obtain the local wind forces in the sway directions (the principal orthogonal axes of the building), the pressure coefficients are multiplied by the associated tributary area for each pressure tap. Note that for each of the pressure tap layouts, the tributary areas were re-defined appropriately to account for the changes in pressure-tap density. Base shears, overturning moments and torsion were computed and converted to their associated coefficients using Eq. (2,3)

$$C_{F_l} = \frac{F_{base\ l}}{0.5\rho B H U_h^2} \qquad with\ l = x, y \tag{2}$$

$$C_{M_l} = \frac{M_{base\ l}}{0.5\rho B H^2 U_h^2} \qquad with\ l = x, y, z \tag{3}$$

where *B* and *H* are the width and height of the building (*B* = 72 m and *H* = 240 m), respectively.

3.3 Dynamic response

Using the results from the wind tunnel tests and modal analysis, the dynamic response of this tall building can be estimated for each of the test wind directions. Because there are eccentricities in the centres of mass of Building A, it will respond to wind excitation with coupled lateral-torsional motions. To increase the efficacy in solving the equations associated with the structural dynamic response, the concept of rigid floor diaphragms has been applied [15] meaning that for each floor plate, the motions are restricted to two translations and one rotation about a vertical axis. The general equation of motion for structures with rigid floor systems under wind load actions can be expressed as:

$$M\ddot{X} + C\dot{X} + KX = W(t) \tag{4}$$

where *M*, *C*, and *K* are the structural mass, damping and stiffness matrices, respectively. *X* is the displacement vector and *W* is the wind load time history vector. Utilising modal analysis and transforming the coupled equations to modal coordinates, a set of uncoupled modal equations can be obtained. Then, they are solved to calculate the final solution.

The dynamic analysis can be carried out in either the time or frequency domains. For this study, time domain dynamic analysis (Newmark method) is used, which has the inherent advantage of capturing the time history of the building responses instead of only statistical values like means and standard deviations which are obtained when frequency domain analysis is used.

To write the codes for doing the calculations and obtaining the results, MATLAB software has been used.

4. Results and Discussion

To examine the influence of pressure-tap resolution on the estimation of the wind-induced loads and dynamic response of the building, the results from the three lower tapping density cases are compared to reference results from the highest pressure-tap density layout (case 1). The Case 1 layout density is close to 120 m^2 per tap, as recommended in the Australasian Wind Engineering Society Quality Assurance Manual. Due to page limitations, only some selected results are presented in this paper.

Time-averaged pressure coefficient distributions with the wind normal to the wide face of the model for the four pressure-tap density cases were calculated and are illustrated as coloured maps in Figure 4. The number of pixels represents the vertical and horizontal variations. The pressure coefficient colour scale is shown on the right. Figure 4 shows that the resolution accuracy reduces from case 1 to case 4. Case 2 appears to have a higher resolution compared to Case 3 because the horizontal pressure gradients are higher than the vertical pressure gradients. Similar trends were evident on the other faces not shown here. Thus, it appears that the horizontal tap density has more effect on the pressure resolution than vertical spacing. A lot of the pressure details are lost in the Case 4 very low density results.

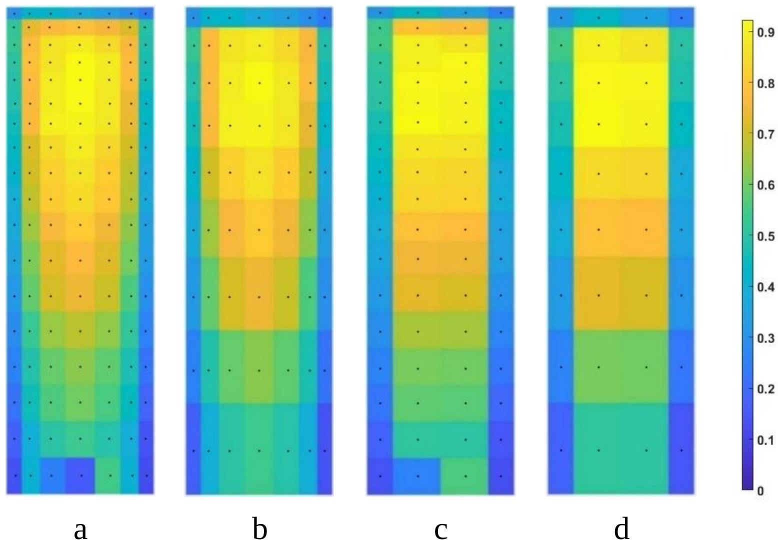

Figure 4. An example of time-averaged pressure coefficient distribution on pressure tap layouts for the case of 0˚ of wind direction: a) Case 1 (18×22), b) Case 2 (9×22), c) Case 3 (18×11), d) Case 4 (9×11).

Figure 5 shows the effect of pressure tap density on selected time history segments of the base overturning moments and torsion coefficients for a wind direction of 40˚. There are no significant differences between the different cases for the base overturning moments (Figure 5a and 5b), while there are considerable differences in torsion (Figure 5c). It can be seen that the results are almost the same for cases 1 and 2 (high horizontal density) and very close for cases 3 and 4 (low horizontal density). Thus, the horizontal variation of the pressure tap density has more effect on torsion than the vertical density. Results from the other wind directions gave similar results. Therefore, in summary Figure 4 and Figure 5 show that the horizontal pressure tap density has significantly more effect on wind-induced loading than the vertical spacing.

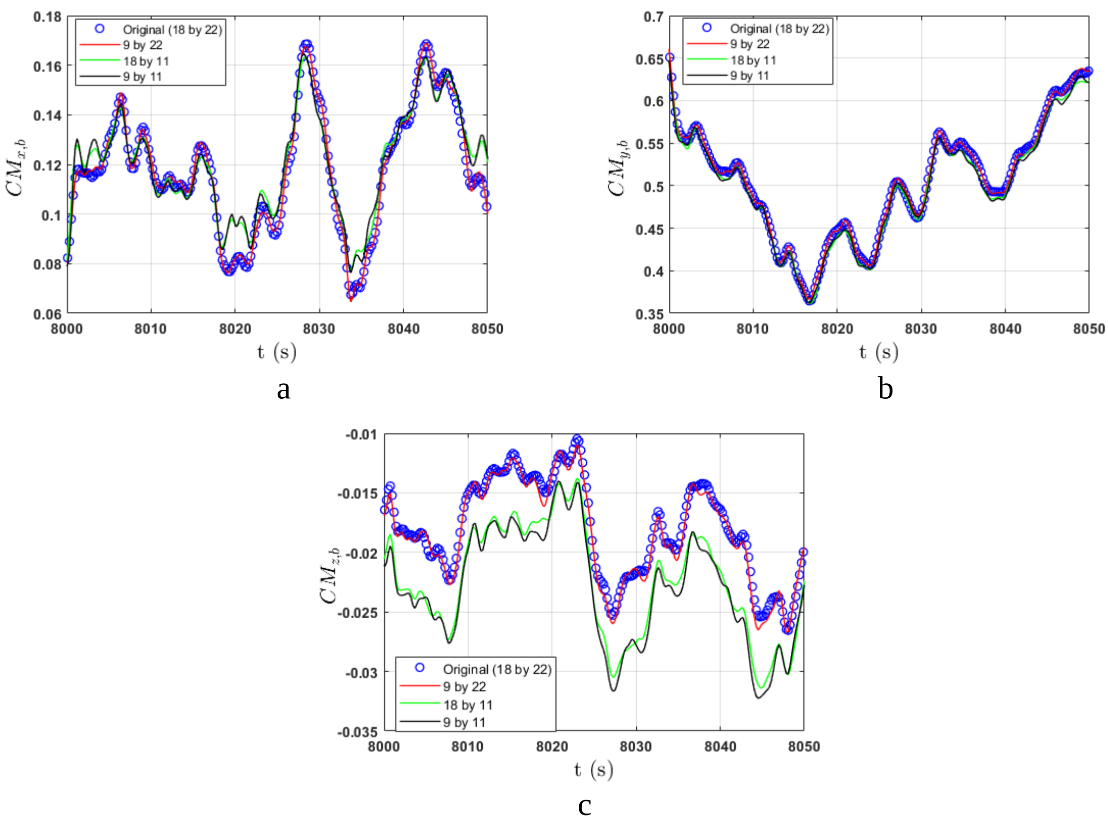

Figure 5. Selected time histories of base sway moments (a and b) and torsion (c) from the four pressure tap layouts at a wind direction of 40˚.

Using time domain dynamic analysis, overturning base moments and torsion coefficients were calculated and the resulting statistical information is summarised in Table 2. It reveals again that the differences are greater when the horizontal spacing is changed in comparison with the vertical spacing, especially for torsion at a wind direction of 40°. Nonetheless, the differences in dynamic response between the four cases are smaller than the aerodynamic results in Figure 5.

C_{M_x}	Wind direction $\theta = 0^\circ$			
	Case 1	Case 2	Case 3	Case 4
Mean	**-0.0038**	**-0.0038**	**-0.0038**	**-0.0039**
Std	**0.0637**	**0.0648**	**0.0636**	**0.0656**
Max	**0.1616**	**0.1637**	**0.1617**	**0.1670**
Min	**-0.1674**	**-0.1713**	**-0.1698**	**-0.1784**

C_{M_x}	Wind direction $\theta = 40^\circ$			
	Case 1	Case 2	Case 3	Case 4
Mean	**0.0686**	**0.0685**	**0.0669**	**0.0665**
Std	**0.0481**	**0.0484**	**0.0445**	**0.0461**
Max	**0.1730**	**0.1757**	**0.1637**	**0.1700**
Min	**-0.0532**	**-0.0557**	**-0.0585**	**-0.0657**

C_{M_x}	Wind direction $\theta = 90^\circ$			
	Case 1	Case 2	Case 3	Case 4
Mean	**0.1408**	**0.1390**	**0.1425**	**0.1400**
Std	**0.0465**	**0.0475**	**0.0499**	**0.0517**
Max	**0.2515**	**0.2551**	**0.2648**	**0.2709**
Min	**0.0413**	**0.0375**	**0.0319**	**0.0248**

C_{M_y}	Wind direction $\theta = 0^\circ$			
	Case 1	Case 2	Case 3	Case 4
Mean	**0.5631**	**0.5629**	**0.5473**	**0.5469**
Std	**0.1505**	**0.1505**	**0.1469**	**0.1471**
Max	**0.8925**	**0.8927**	**0.8698**	**0.8705**
Min	**0.2428**	**0.2412**	**0.2331**	**0.2312**

C_{M_y}	Wind direction $\theta = 40^\circ$			
	Case 1	Case 2	Case 3	Case 4
Mean	**0.4441**	**0.4417**	**0.4426**	**0.44**
Std	**0.1195**	**0.1188**	**0.1178**	**0.1171**
Max	**0.6921**	**0.6876**	**0.6855**	**0.6812**
Min	**0.3178**	**0.3177**	**0.3127**	**0.3116**

C_{M_y}	Wind direction $\theta = 90^\circ$			
	Case 1	Case 2	Case 3	Case 4
Mean	**-0.0078**	**-0.0086**	**-0.0085**	**-0.0102**
Std	**0.1567**	**0.1609**	**0.1767**	**0.1829**
Max	**0.3578**	**0.3722**	**0.4091**	**0.4273**
Min	**-0.3717**	**-0.3845**	**-0.4257**	**-0.4378**

C_{M_z}	Wind direction $\theta = 0^\circ$			
	Case 1	Case 2	Case 3	Case 4
Mean	**-0.0183**	**-0.0180**	**-0.0178**	**-0.0176**
Std	**0.0099**	**0.0101**	**0.0098**	**0.0102**
Max	**0.0058**	**0.0071**	**0.0062**	**0.0075**
Min	**-0.0437**	**-0.0440**	**-0.0433**	**-0.0441**

C_{M_z}	Wind direction $\theta = 40^\circ$			
	Case 1	Case 2	Case 3	Case 4
Mean	**-0.0259**	**-0.0254**	**-0.0291**	**-0.0286**
Std	**0.0077**	**0.0078**	**0.0083**	**0.0084**
Max	**-0.0085**	**-0.0075**	**-0.0107**	**-0.0095**
Min	**-0.0281**	**-0.0289**	**-0.0336**	**-0.0348**

C_{M_z}	Wind direction $\theta = 90^\circ$			
	Case 1	Case 2	Case 3	Case 4
Mean	**0.0026**	**0.0025**	**0.0026**	**0.0024**
Std	**0.0126**	**0.0132**	**0.0161**	**0.0171**
Max	**0.0359**	**0.0376**	**0.0469**	**0.0491**
Min	**-0.0319**	**-0.0338**	**-0.0417**	**-0.0448**

Table 2. Statistical data of base overturning moments and torsion coefficients from dynamic analysis for different pressure layouts and wind directions.

Table 3 presents the peaks of the resultant tip acceleration at the corner, and tip displacement in the *x* and *y* directions for different wind directions. It shows that the horizontal pressure tap density has a more significant effect on the tip acceleration and displacement peaks in comparison with vertical spacing. In fact, the results with the same horizontal pressure tap density are very close. The present results show much larger values of tip displacements and accelerations when the horizontal spacing is low and are presumably overestimating the responses.

$\boldsymbol{\theta = 0^\circ}$	Tip resultant acceleration (mg)	Tip displacement (m)	
		X direction	Y direction
Case 1	**32.37**	**0.4542**	**0.0237**
Case 2	**33.11**	**0.4426**	**0.0239**
Case 3	**63.23**	**0.8423**	**0.0449**
Case 4	**65.34**	**0.8212**	**0.0462**

$\boldsymbol{\theta = 40^\circ}$	Tip resultant acceleration (mg)	Tip displacement (m)	
		X direction	Y direction
Case 1	**23.13**	**0.3576**	**0.0074**
Case 2	**23.36**	**0.3556**	**0.0081**
Case 3	**44.32**	**0.6603**	**0.0144**
Case 4	**46**	**0.657**	**0.0166**

$\boldsymbol{\theta = 90^\circ}$	Tip resultant acceleration (mg)	Tip displacement (m)	
		X direction	Y direction
Case 1	**39.94**	**0.182**	**-0.0067**
Case 2	**56.7**	**0.2070**	**-0.0056**
Case 3	**81.52**	**0.3507**	**-0.0116**
Case 4	**113.92**	**0.398**	**-0.0089**

Table 3. Peaks of tip accelerations and tip displacement for the four pressure tap densities for three wind directions.

5. Conclusions

The number of pressure taps in the HFPI approach can influence the structural wind response accuracy. In this experimental and analytical study, using four different pressure tap layout densities, the effect of pressure tap density on the prediction of wind-induced loads and dynamic response are examined for Building A, a benchmark tall building used in wind engineering. The results demonstrate that the horizontal tap density has significantly more effect on the pressure resolution on the surfaces of the model and the wind-induced loads than the vertical spacing. This result is not unexpected as the horizontal pressure gradients on buildings are higher compared to the vertical direction. Examining the base sway moments and torsion results shows that the base torsion has the highest sensitivity to the pressure tap density. Utilising time domain dynamic analysis, the peak tip accelerations at a corner, and tip displacements in the sway directions were computed. It is found that horizontal variation in pressure tap density has a more significant effect on the results than the vertical variation. Comparing results with the Australasian Wind Engineering Society Quality Assurance Manual, it seems that a maximum area of 120 m^2 per tap is an appropriate recommendation.

References

1. Holmes, J., Tse, K., Ho, T., and Boggs, D. *Benchmark buildings for high-frequency base balance tests*. in Proceedings of the 4th International Conference on Advances in Wind and Structures (AWAS-08). 2008. Jeju, Korea.
2. Holmes, J.D. and Tse, T.K., International high-frequency base balance benchmark study. Wind and Structures, 2014. 18(4): p. 457-471.
3. AWES, Quality Assurance Manual for Wind-Engineering Studies of Buildings. AWES-QAM-1-2019.
4. Salehinejad, M.M. and Flay, R.G.J., A review of approaches to generate equivalent static and synthetic wind loads on tall buildings for the preliminary stage of design. Journal of Wind Engineering and Industrial Aerodynamics, 2021. 219: p. 104823.
5. Salehinejad, M.M. and Flay, R.G.J., Generating equivalent static wind loads for a tall building using base moment spectra, in 22nd Australasian Fluid Mechanics Conference AFMC2020. 2020, The University of Queensland: Brisbane, Australia.
6. Park, S. and Yeo, D., Effects of aerodynamic pressure tap layout and resolution on estimated response of high-rise structures: A case study. Engineering Structures, 2021. 234: p. 111811.
7. Simiu, E. and Yeo, D., Wind effects on structures: Modern structural design for wind. 4th ed. 2019: John Wiley & Sons.
8. Dragoiescu, C., Garber, J., and Kumar, K.S. A Comparison of force balance and pressure integration techniques for predicting wind-induced responses of tall buildings. in Structures Congress 2006: Structural Engineering and Public Safety. 2006.
9. TPU. Tokyo Polytechnic University (TPU) aerodynamic database. Available from: http://wind.arch.t-kougei.ac.jp/system/eng/contents/code/tpu.
10. ASCE, Wind tunnel testing for buildings and other structures. ASCE 49-12, 2012.
11. Melbourne, W., Comparison of measurements on the CAARC standard tall building model in simulated model wind flows. Journal of Wind Engineering and Industrial Aerodynamics, 1980. 6(1-2): p. 73-88.
12. Dragoiescu, C., Suresh Kumar, K., and Garber, J. Tap Resolution Related to the Accuracy of Pressure Integrated Wind Loads. in 5th European & African conference on wind engineering. 2009. Florence, Italy: Firenze University Press.
13. AS/NZS 1170.2: 2021 Structural design actions-Part 2: Wind actions. 2021.
14. Salehinejad, M.M., Li, Y.F., Ma, Q., and Flay, R.G.J., A comparison of force balance and pressure integration techniques for predicting wind-induced and dynamic responses of tall buildings, in 23rd Australasian Fluid Mechanics Conference AFMC2022. 2022, The University of Sydney: Sydney, Australia.
15. Clough, R.W. and Penzien, J., Dynamics of structures. 1993: MacGraw-Hill.